Micromixing and microchannel design: vortex shape and entropy

Francesco M. MASTRANGELO[1*], Francesco PENNELLA[1], Filippo CONSOLO[1],
Marco RASPONI[2], Alberto REDAELLI[2], Franco M. MONTEVECCHI[1], Umberto MORBIDUCCI[1]

- Corresponding author: Tel.: ++39 (0)11 5646969; Fax: ++39 (0)11 5646999;
  - Email: francesco.mastrangelo@polito.it

1: Department of Mechanical Engineering, Politecnico di Torino, IT
2: Department of Biomedical Engineering, Politecnico di Milano, IT

Abstract In very recent years microdevices, due to their potency in replacing large-scale conventional laboratory instrumentation, are becoming a fast and low cost technology for the treatment of several chemical and biological processes. In particular microfluidics has been massively investigated, aiming at improving the performance of chemical reactors. This is because of the fact that reaction is often an interface phenomenon where the greater the surface to volume ratio, the higher the reaction speed, and microscale mixing increases the interfacial area (in terms of mixing-induced-by-vortices generation). However, microfluidic systems suffer from the limitation that they are characterized mostly by very low Reynolds numbers, with the consequence that (i) they cannot take advantage from the turbulence mixing support, and (ii) viscosity hampers proper vortex detection. Therefore, the proper design of micro-channels (MCs) becomes essential. In this framework, several geometries have been proposed to induce mixing vortices in MCs. However a quantitative comparison between proposed geometries in terms of their passive mixing potency can be done only after proper definition of vortex formation (topology, size) and mixing performance. The objective of this study is to test the ability of different fluid dynamic metrics in vortex detection and mixing effectiveness in micromixers. This is done numerically solving different conditions for the flow in a classic passive mixer, a ring shaped MC. We speculate that MCs design could take advantage from fluidic metrics able to rank properly flow related mixing.

Keywords: Entropy, Helicity, Mixing, Vortex identification

1. Introduction

The possibility to replace large-scale conventional laboratory instrumentation with miniaturized systems offers a variety of advantages, including reduced hardware costs, low reagent consumption and faster analysis. In this circumstance, microfluidics is becoming a key technology in many chemical, biochemical, and biological applications. In fact, microfluidic systems are compact in size, disposable, and ensure high speed of analysis using decreased sample volumes.

It is well known that at the micro scale mixing becomes crucial to optimize the performance of chemical reactions (Hessel and Löwe and Schönfeld 2005, Stroock et al. 2002, Whitesides 2006).

In general, mixing strategies can be classified as either active or passive, according to the operational mechanism. Active mixers employ external forces in order to perform mixing. On the contrary, passive mixers avoid resorting to external electrical or mechanical sources by exploiting characteristics of specific flow fields in channel geometries to mix species. As microfluidic systems are characterized mostly by laminar, very low Reynolds flows, they cannot take advantage of turbulence in order to enhance mixing. In the absence of turbulence mixing support, the design of micro-channels (MCs) acting as micromixers becomes essential, in terms of properly induced vortices. Vortices are effective in both chemicals and heat diffusion processes: vortices fold the fluid stream increasing the area interested in diffusion and reducing diffusion boundary layer thickness. Several geometries for MCs have been proposed to induce mixing, with ribs, wedges, or abrupt turns used to elicit vortices (Hessel and Löwe and Schönfeld 2005, Stone and Stroock and Ajdari, 2004). Hence, from the previous

remarks, it is clear that when micromixing is needed, a comparison between MCs designs must be done in terms of their capability of vortex formation at low Reynolds numbers.

The objective of this study is to compare the capability of different fluid dynamic metrics in estimating the performance both in vortex detection and mixing effectiveness of micromixers. This is done simulating different conditions for the flow, by means of the finite volume method, in a ring shaped MC, where centrifugal effects could induce secondary flows characterized by the presence of counter-rotating vortices (located in transversal sections of the channel).

The MC geometry here considered serves to define proper vortex identification performances in terms of topology, number and mixing potency.

2.   Methods

In this study, we used a ring shaped, square section duct geometry of MC, like the one previously proposed by Schonfeld and Hardt (2004) (Fig. 1).
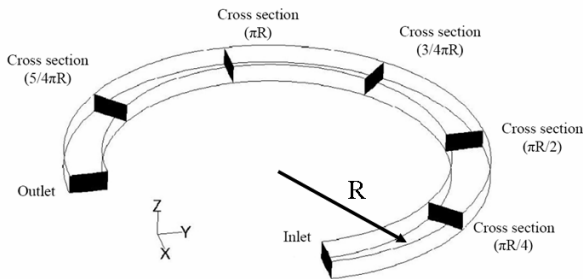

Fig. 1. Square duct used to elicit twin vortices formation as due to Dean curvature instability. Computational domain and volume sections for vortex detection.

This undemanding geometry, characterized by a constant curvature, induces the formation of secondary vortices in consequence of centrifugal forces arising at certain flow conditions. Dean (1928) proved that the flow confined between two cylinders undergoes secondary flow formation when the dimensionless Dean number Dn

$$Dn = \frac{u_0 D}{\nu}\sqrt{\frac{D}{R}} = \mathrm{Re}_D\sqrt{\kappa D} \quad (1)$$

exceeds a threshold of about 36, where Re_D is

diameter based Reynolds number, D is the hydraulic diameter, u_0 the averaged velocity, ν the fluid kinematic viscosity, k the duct curvature (kD nondimensional curvature), R is the ring radius (equal to $5D$ in our simulation).

Dean number is a bifurcation parameter for the non linear Navier Stokes equations: beyond Dean threshold fluid evolves vortices. Dean proved that the flow undergoes a progressive centrifugal displacement of the maximal axial velocity, leading to the onset of vortices because of the unbalance of the centrifugal force and radial gradient of static pressure.

Governing equations and computational model

The numerical results presented in this work were based on the solution of the incompressible Navier–Stokes equations and the convection–diffusion equation for a concentration field by means of the finite volume method: computed Knudsen number confirms the appropriateness of continuum mechanics approach. In this work, like in Schonfeld and Hardt (2004), we were mainly interested in the convective patterns redistributing the liquid transverse to the flow direction. With this analysis we aimed at obtaining information on the characteristic dimensions of the lamellae and the mixing length to be expected. Flow was assumed steady and laminar. Hence, the flow motion governing equations and convection–diffusion equation are:

$$\nabla \cdot \boldsymbol{v} = 0 \quad (2)$$

$$\rho(\boldsymbol{v}\cdot\nabla)\boldsymbol{v} = -\nabla p + \mu\nabla^2\boldsymbol{v} \quad (3)$$

$$\frac{\partial c}{\partial t} + (\boldsymbol{v}\cdot\nabla)c = D\nabla^2 c \quad (4)$$

where $\boldsymbol{v}$ and p are the velocity vector and the pressure in each point of the fluid domain, respectively; ρ and μ are fluid density and viscosity, respectively; D is the diffusion coefficient and c denotes concentration. For the reason mentioned above and in accordance with Schonfeld and Hardt (2004), here the inter species diffusion coefficient D was set equal to zero: eq. (4) states that the species concentration is constant along each streamline. Both the MC geometry and the

computational grid were created with the solid modeller GAMBIT (ANSYS Inc.). A structured mesh of about 200,000 hexahedral cells was used (in consequence of a mesh sensitivity analysis). A flat velocity profile was imposed at the inlet section of the duct while at the outlet pressure reference value was prescribed. No slip conditions were prescribed at duct walls. The adopted boundary conditions made the geometric symmetry plane a fluid dynamic symmetry plane: this allowed to study only half of the fluid domain. Ten simulations were performed at different Re_D numbers (linear range 2.24-224, corresponding to Dn range 1-100) using the commercial solver Fluent (ANSYS Inc). The SIMPLEC algorithm was used for pressure–velocity coupling, and the QUICK differencing scheme was used for discretization of the species concentration. The second order and the second order upwind differencing schemes were used for velocities and pressure fields, respectively.

Vortex identification

Velocity and concentration fields were further post processed in Matlab environment (Mathworks Matlab Inc.) for vortex identification and mixing quantitative evaluation. Considering the remarks on the role played by secondary vortices in micromixing, we remind here that Jeong and Hussain (1995) stated that a vortex should posses at least two properties:

• the vortex core should have net circulation (no potential flows);

• the geometrical characteristics of an identified vortex core should be Galilean invariant.

In a purely rotational motion the flow undergoes a rigid body rotation: in this region the absence of strain prevents stream from blending. Thus, a vortex core can be defined as the rotational part of the vortex, while out of this region the vorticity decreases, eliciting stream folding and related mixing.

For evaluating mixing, vortex identification is mandatory, even if unambiguous, universal methods are still lacking: plausibly vortex is a connected region of finite volume where vorticity is spatially correlated. As a consequence, vortex identification methods based on local quantities are preferable to particle-based methods (Cucitore and Quadrio and Baron 1999). In this study, we applied one of the mainly adopted vortex detection methods, which are based on velocity gradients (i.e., based on local quantities). The λ_2-method was introduced by Jeong and Hussain (1995). It defines the vortex as a region of negative values of the scalar λ_2 (second eigenvalue of the tensor $S^2 + \Omega^2$, respectively symmetric and antisymmetric parts of velocity gradient ∇u), measure of balance of flow strain and rotation in uncompressible flows (Cucitore et al. 1999, Jeong and Hussain 1995). When λ_2 is negative, at least two eigenvalues are negative therefore fluid undergoes swirling motion.

Topology of the flow: helicity

Moffatt (1969) introduced into the fluid mechanics literature the term "helicity" as the degree at which the velocity field lines wrap and coil around each other. The helicity H(t) of a fluid flow confined to a three dimensional domain D (bounded or unbounded) of volume V is defined as:

$$H = \int_V V \cdot (\nabla \times V) dV \qquad (5)$$

The pseudoscalar quantity H_k, given by the inner product of the velocity **V** and vorticity **ω** fields (**ω** $= \nabla$ x **V**):

$$H_k = V \cdot (\nabla \times V) \qquad (6)$$

is the helicity density per unit volume. Helicity admits topological interpretation in relation to the linkage of vortex lines of the flow, thereby, just like energy, it has a great influence on the evolution and stability of both laminar and turbulent flows. In non potential flows Eq. (6) states that: (i) H_k is maximal in module (for a given total kinetic energy) when velocity (**V**) and vorticity (**ω**) vectors lie along the same direction (i.e., $/H_k/ = |$**V**$| |$**ω**$|$); (ii) the flow has a null helicity density value when velocity or vorticity go to zero or when velocity (**V**) and vorticity (**ω**) lie along orthogonal directions (i.e., $H_k = 0$). Considering the remarks on

helicity, it is possible to define the basic quantity local normalized helicity:

$$LNH = \frac{\mathbf{V} \cdot (\nabla \times \mathbf{V})}{|\mathbf{V}||(\nabla \times \mathbf{V})|} \qquad (7)$$

The quantity *LNH* is the local value of the cosine of the angle between the velocity and vorticity vectors. According to Eq. (7), *LNH* is one in module when the flow is purely helicoidal and zero when the flow is purely axial, circumferential or, in general, when either vorticity is null or orthogonal to velocity. In this work, we used the scalar *LNH* to calculate on sections of the MC transversal to its axis (cross-sections) a basic metric, the Normalized Average Helicity (NH$_{avg}$):

$$NH_{avg} = \frac{1}{S} \int_S \left| \frac{\mathbf{V} \cdot (\nabla \times \mathbf{V})}{|\mathbf{V}||(\nabla \times \mathbf{V})|} \right| dS \qquad (8)$$

where S is the area of the transversal section of the MC. The average surface integral of the absolute value of LNH was computed on seven sections of the MC (see fig. 1).

Measure of mixing: Shannon Entropy

The entropy concept was introduced as a measure of mixing by Wang et al. (2003). Similarly to Kang and Kwon (2004), we calculated information entropy as a quantitative measure of mixing, using coloured particles to visualize mixing in the MC, being the distribution of coloured particles related to the degree of mixing. To do this, we seeded the inlet section of the MC with a cluster of N=45000 binary coloured inert particles. The two non mixable species define an interface which develops flowing through the MC. Like in Kang and Kwon (2004), for a certain particle configuration of multiple species, the mixing entropy (S) is defined as a sum of the information entropy of individual cells constituting a cross-sectional area of the MC:

$$S = \sum_{i=1}^{Nc} \left[w_i \sum_{k=1}^{Ns} \left(n_{i,k} \log n_{i,k} \right) \right] \qquad (9)$$

where *i* is the index for the cell, *k* is the index for the species, w_i is the weighting factor for the cell, *Nc* is the number of cells, N_s is the number of species to be mixed (two in our case) and $n_{i,k}$ is the particle number fraction of the k_{th} species in the i_{th} cell. The weighting factor, w_i, is devised such that it is set to be zero for a cell with no particles at all or including only a sole species.

Reasonably, the mixing entropy increases along the downstream direction, if the MC flow conditions allows vortex generation. The ratio of entropy increment k_{SE} (ratio between entropy gain and maximal entropy difference) serves as an indicator of achievable mixing:

$$k_{SE} = \frac{S - S_0}{S_{max} - S_0} \qquad (10)$$

Eq. (10) states that k_{SE} is defined as the ratio of the entropy gain at a certain location to the maximum possible entropy increase: a k_{SE} value equal to 1 corresponds to the maximal disorder (independently to cell size), i.e., a condition of uniform particle distribution of all the different specimens, while k_{SE} equal to 0 corresponds to maximal order or zero mixing as the one at the inlet. Cross sectional cell division for entropy calculation was set accordingly to the principle proposed by Schonfeld and Hardt (2004).

3. Results

In the range of Reynolds numbers of interest for MCs, the fluid behaves as dominated by the viscous term. Non slip condition at the duct wall induces vorticity: the boundary layer bears the mainstream acting as a distributed bearing. This generates a vortex ring coupled within the duct walls. This vortex ring does not elicit mixing. Furthermore, in this boundary layer wall induced vorticity represents a bias in the vorticity field we are interested in, thus preventing from the proper detection by of expected streamwise vortex twins (Cucitore et al. 1999).

At low Reynolds (and Dean as a consequence in our case, see equation 1), numbers λ_2 detects vortices located near the inner wall of the duct. As an example, figure 2 (upper panel) shows that at *Dn* = 10 (*Re$_D$* = 22.4) the distribution of negative values of λ_2 is placed towards the inner wall of the MC, and spans up to the fluid dynamic symmetry plane, failing in identifying the cores of the vortices,

as can be easily observed looking at the velocity vector map.

Figure 2 (lower panel) also puts in evidence that at higher Dean numbers (*Dn*=50; $Re_D = 111.8$), the scalar λ_2 (λ_2 scales as $(u_0/D)^2$) identifies a couple of counter-rotating vortex twins which interact at symmetry plane of the channel.
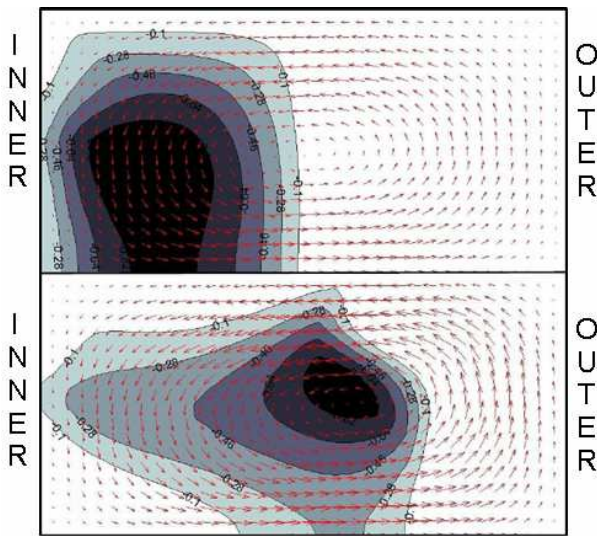

Fig. 2. Contour plot of the λ_2 scalar at different Dean number (*Dn* = 10, 50 up and down respectively) for plane πR from the inlet. The section minima for λ_2 scalar are respectively -3.0E5 s^{-2}, -1.1E7 s^{-2} for *Dn* = 10, 50.

Figures 3, 4 display contour maps of the helicity density over the cross section at distance πR from the inlet of the MC, at *Dn* numbers equal to 10 and 50, respectively. By definition, H_k is a pseudo scalar and is antisymmetric with respect to the symmetry plane. Notably, H_k is null at the duct walls and at the symmetry plane, where velocity and vorticity are orthogonal to each other, thus giving demonstration of its ability in defining vortex twins detached from symmetry plane. We observe, at all *Dn* (Re_D) numbers in the range here investigated, the presence of a well localized stationary point for H_k (respectively a maximum or a minimum in the two halves of the MC, with respect to the symmetry plane), at all the MC cross sections. At low *Dn* numbers this helicity density stationary point is located at the duct cross section centre (Fig. 3, upper panel), and it moves towards the outer wall (consequence of centrifugal velocity peak value displacement) as the *Dn* number

increases (Fig. 4, upper panel). Interestingly, we observe that: (i) the localized stationary point of H_k identifies unambiguously the core of the vortex over MC cross sections at low Dean number, as it can be easily observed looking at the velocity vector map (figure 3, upper panel); (ii) the cross sectional position of the stationary point value of H_k moves according to the peak value of the velocity vector component normal to the cross section, as shown in figures 3 an 4 (lower panel).
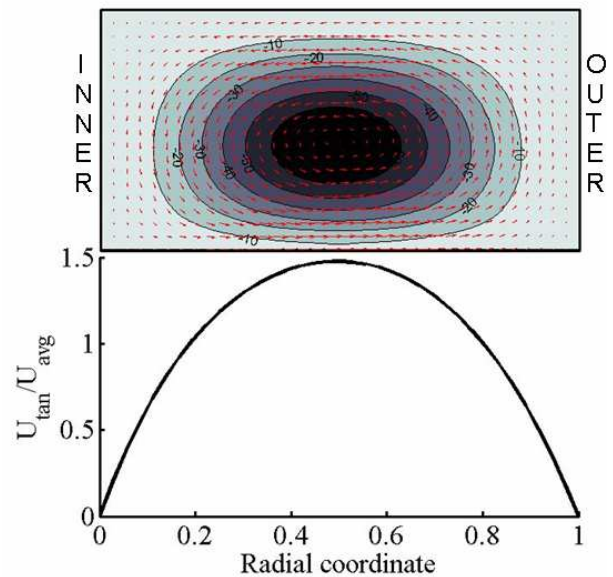

Fig. 3. Cross section πR. Helicity density distribution (in ms^{-2}) at *Dn* =10. Velocity profile at the fluid symmetry plane. At low Re_D numbers the profile of the velocity component normal to the cross section is insensible to duct curvature, therefore it's about symmetrical to local vertical plane. On the symmetry plane vorticity and velocity are orthogonal, therefore H_k.is null.

A qualitative visualization of the vortex related mixing is given by the color distribution of the two non mixable species over MC cross sections. The seeded particles, mimicking the two species, belong respectively to the intrados (red particles) and extrados (black particles) part of the inlet section (Fig. 5, upper panel). As an example of what we observed, we report in figure 5 the results obtained at *Dn*=20 (Re_D = 44.7): the initial vertical interface between non mixable species folds, in MC cross section downstream of the inlet section, increasing the interface area.
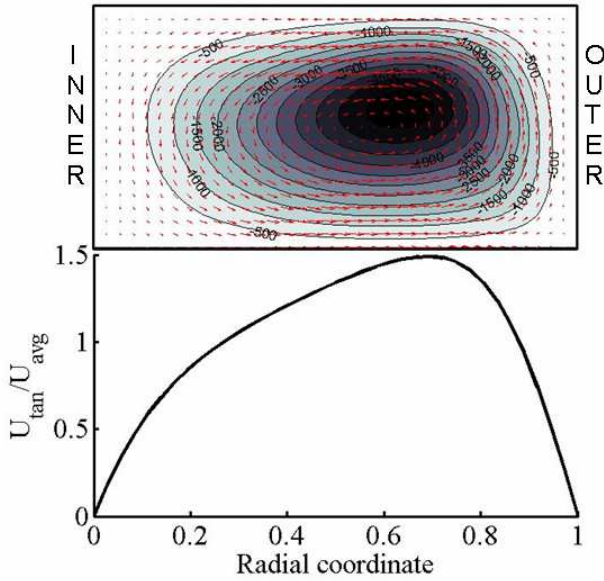
Fig. 4.Cross section πR. Helicity density distribution (in ms^{-2}) at $Dn = 50$. Velocity profile at the fluid symmetry plane. The increment of Reynolds number, and relate increment in Dean number, induces a centrifugal skewness in the velocity profile. Helicity density H$_k$, zeroed at the fluid symmetry plane, shows a minimum displaced radially.

In fact, evaluating the particle distributions at successive cross sectional locations, the color pattern changes from the initial distribution: for *Dn*=20 the stream folding is limited, but the interface increases because of stretching, folding of the fluid with a resulting thinning of the diffusion boundary layer (Fig. 5). We noticed from qualitative visualizations that the stream folds more as *Dn* number increases, as shown in Fig. 6, where species distribution is depicted at the same MC cross section (at a distance equal to πR from the inlet section), at *Dn* numbers equal to 10 (left panel) and 50 (right panel).

Figure 7 displays the values assumed by the normalized average helicity NH$_{avg}$ over MC cross sections along the duct, at two *Dn* numbers.

It is possible to notice that (i) as Dean number increases, NH$_{avg}$ increases over the same MC cross section, (ii) NH$_{avg}$ exhibits a plateau at a certain distance from the inlet section, due to the similarity of fluid flow along the streamwise cross sections, putting in evidence a progressive realignment of vorticity in streamwise direction.
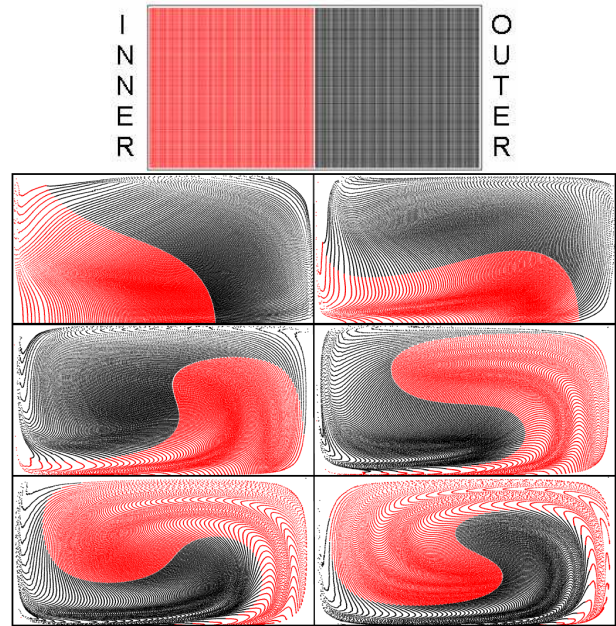

Fig. 5. Shannon entropy colored map at different plane (inlet and cross section at π/4R, π/2R, 3/4πR, πR, 5/4πR, 3/2πR) for *Dn*=20.
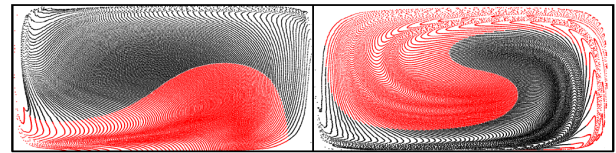

Fig. 6. Shannon entropy colored map at different Dean number (*Dn* =10, 50 on the left and right respectively) for cross section πR

$$NH_{avg} = \frac{1}{S} \int_{S} \left| \frac{\mathbf{V} \cdot \boldsymbol{\omega}}{\|\mathbf{V}\| \|\boldsymbol{\omega}\|} \right| dS$$
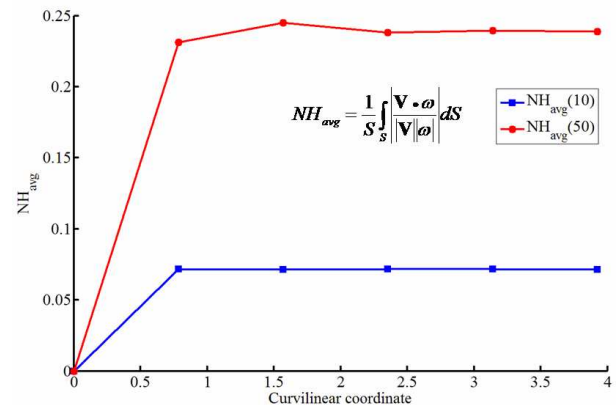
Fig. 7 Half section average helical density (NH$_{avg}$). The NH$_{avg}$ shows a plateau for the similarity of fluid flow along the stream wise sections. Greater is the NH$_{avg}$ higher is the entropy increment gain going streamwise.

Figure 8 displays the values assumed by the Shannon entropy ratio k_{SE} over MC cross sections along the duct, at two *Dn* numbers. It can be noticed that k_{SE} increases moving away from the inlet section with an increment more marked for the highest *Dn* numbers.
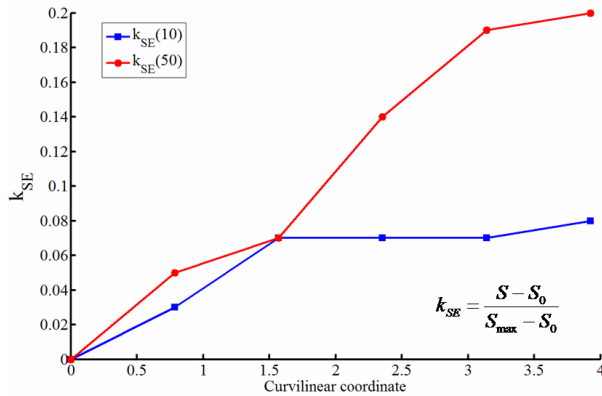
Fig. 8 Entropy increment ratio (k_{SE}). Stream wise k_{SE} increases more markedly as Dean number increases. Greater is the NH_{avg} higher is the entropy increment gain going streamwise.
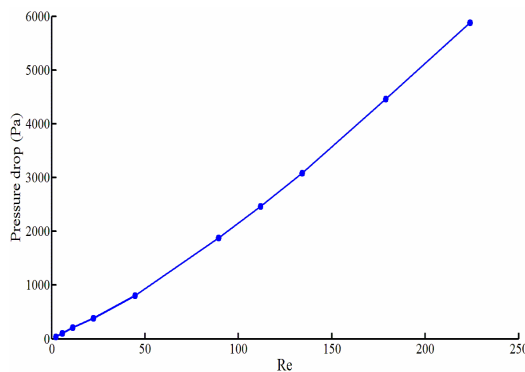

Fig. 9 Pressure drop along the pipe as a function of Re_D.

In accordance with Dean (1928) we observed that the presence of secondary vortices has a marginal effect on energy dissipation when compared to hydraulic energy losses in straight conduits at low Reynolds numbers (see the linear behavior of pressure drop along the duct vs Re_D in fig. 9).

4.Discussion

Consistently to vortex definition criteria, the presence of a fluid dynamic symmetry plane forces vortex twins to be expected. In fact fluid is symmetric with respect of duct spanning plane: a even number of vortices detected by identification methods is expected. From a phenomenological viewpoint, we know that proper vortex identification methods were developed at high Reynolds numbers by several authors, making use of velocity field derived scalars, pressure scalars and particles tracking techniques. However at low Reynolds numbers, i.e. the working flow regimes in MCs, viscosity hampers proper vortex detection (Cucitore et al. 1999). This difficulty

in methods for vortex detection at the flow regimes at which MCs operate becomes, as a consequence, a limitation in properly setting design strategies for micromixing enhancement, where passive mixing is based on induction of secondary vortices in MCs.

As reported by other authors (Siggers and Waters 2005), flow undergoes vortices formation even at sub critical values of Dean number (for infinite cylinders $Dn_{cr} \cong 36$, Dean 1928). Vortices develop from the inlet as velocity maximum is displaced centrifugally: the progressive velocity displacement induces recirculation and vortex twins (Siggers and Waters 2005). In this vortex induction process, duct curvature is the key factor. At low Re_D this process is limited and fluid pattern behaves similarly to the one typical of straight duct. The viscous term dominates the flow as shown in microfluidic system: for the curved channel considered here, at values of Re_D lesser than 2.25 ($Dn = 1$) the velocity field is about symmetric and the centrifugal effects are damped. Hence, duct curvature has a marginal effect on centrifugal displacement of velocity maximum.

Vorticity norm is unsuitable in vortex identification: shear induces vorticity which prevents from the proper vortex identification. The high value of vorticity induced by this creeping flow biases the vorticity norm, preventing from the identification of local vorticity stationary point expected in vortex cores. The λ_2 method is more effective for vortex detection in the boundary layer of the innner wall (fig. 2). However the λ_2–based definition of a vortex, defined from isosurfaces of λ_2, at low Dn numbers could be misleading in identifying vortex twins, since λ_2 iso-surfaces intersect the symmetry plane, in curved MCs. This could lead both to incorrect design and mixing evaluation.

Our results confirm previous general observations relative to similar scalars for vortex detection, in flows dominated by the viscous term (Cucitore et al. 1999): at low Re_D numbers (representing a range of working conditions for MCs), no proper value for the λ_2 scalar was found able to detect vortex twins. In a different way, we observe that

mapping helicity density allows vortex core detection identification in MCs working flow regimes (see figure 3). Moreover, being helicity a pseudoscalar, it serves in detecting couple of vortex twins rotating in opposite directions.

The color distribution of two non mixable species over MC cross sections puts in evidence that the straight interface at the inlet section develops showing stream folding and thinning of lamellae (fig. 5). This phenomenon is limited but not negligible at low Dean numbers, while at a higher Dean numbers interface distortion is more marked (fig. 6) resulting in a increased stream folding (secondary flow).

The entropy-based metric k_{SE}, a measure of the mixing over MC cross sections, increases faster along the curvilinear length of the MC, putting in evidence that mixing increases moving away from the inlet section, with a rate depending on the Dean number: the greatest *Dn*, the higher the mixing over the MC cross section (fig. 8).

As for the helicity-based metric NH_{avg}, it increases steeply just downstream of the inlet section (due to curvature), rapidly reaching a plateau. Interestingly, NH_{avg} values increase with the Dean number.

In conclusion, we found that helicity density is promising in proper vortices detection at low values for Re_D: a curved microchannel geometry served to test vortex identification methods and mixing performance. We speculate that micromixer design could gain more precise insight on vortex topology from the proposed scalar.

In the future, the metrics herein applied to a simple model of MC will be used to test the mixing potency of innovative designs of MCs. Moreover the interplay between Reynolds number and no dimensional curvature in micro fluidic system will be analyzed in the framework proposed by Dean.

References

Cucitore, R., Quadrio, M., Baron, A., 1999. On the effectiveness and limitations of local criteria for the identification of a vortex. European Journal of Mechanics - B/Fluids Volume 18, Issue 2, Pages 261-282.

Dean, W. R., 1928. Fluid Motion in a Curved Channel. Proceedings of the Royal Society of London. Volume 121, Issue 787, pp. 402-420.

Hessel, V., Löwe, H., Schönfeld F., 2005. Micromixers—a review on passive and active mixing principles. Chemical Engineering Science, Volume 60, Issues 8-9, April-May 2005, Pages 2479-2501

Jeong, J. and Hussain, F., 1995. On the identification of a vortex. Journal of Fluid Mechanics, 285:69-94.

Kang, T. G., Kwon, T.H., 2004. Colored particle tracking method for mixing analysis of chaotic micromixers. Journal of Micromechanics and Microengineering 14, 891.

Moffat, H.K., 1969. The degree of knottedness of tangled vortex lines. J. Fluid Mech. 35, 117-129.

Schöenfeld, F., and Hardt, S., 2004. Simulation of Helical Flows in Microchannels. AIChE Journal, Vol. 50, No. 4, pp. 771-778.

Siggers, J. H., and Waters, S. L., 2005. Steady flows in pipes with finite curvature. Physics of Fluids, Volume 17, Issue 7, pp. 077102-077102-18.

Stone, H. A., and Stroock, A. D., and Ajdari, A., 2004. Engineering flows in small devices: microfluidics toward a lab-on-a-chip. Annual Review of Fluid Mechanics, 2004, 36, 381-411.

Stroock, A.D., Dertinger, S.K.W., Ajdari, A., Mezic, I., Stone, H.A., Whitesides, G.M., 2002. Chaotic Mixer for Microchannels. Science, 295, 647-651.

Sudarsan, A. P., and Ugaz, V. M., 2006. Multivortex micromixing. Proceedings of the National Academy of Science, vol. 103, Issue 19, p.7228-7233.

Wang. W, and Manas-Zloczower, I. and Kaufman, M., 2003. Entropic characterization of distributive mixing in polymer processing equipment. AIChE J. 49 1637–44.

Whitesides, G. M., 2006. The origins and the future of microfluidics. Nature 442, 368-373.